

Charm Leptonic and Semileptonic Decays

P. Zweber^a

^aUniversity of Minnesota, Minneapolis, Minnesota 55455 USA

Experimental results for the pseudoscalar decay constants f_D and f_{D_s} are reviewed. Semileptonic form factor results from $D \rightarrow (\text{pseudoscalar})l\nu$ and $D \rightarrow (\text{vector})l\nu$ decays are also reviewed.

1. INTRODUCTION

The study of charmed meson decays are important for improving our knowledge of the Standard Model (SM). In particular, the study of leptonic and semileptonic decays allow us to measure the CKM matrix elements V_{cs} and V_{cd} to a high level of precision. Leptonic and semileptonic decays are also used to test theoretical predictions describing the strong interaction (QCD) in heavy quark systems. Charmed meson decays are a good laboratory to test Lattice QCD (LQCD) predictions, which can then be applied with confidence to bottom meson decays. Improved theoretical predictions will not only lower the uncertainty in the CKM matrix elements mentioned above but also V_{cb} and V_{ub} .

2. LEPTONIC DECAYS

Leptonic decays of heavy mesons involve the annihilation of the constituent quarks into a neutrino and charged lepton via a virtual W boson. The probability for the annihilation is proportional to the wavefunctions of the quarks at the point of annihilation and is incorporated within the decay constant of the meson. The leptonic decay partial width of the $D_{(s)}^+$ meson within the SM is given by [1]

$$\Gamma(D_{(s)}^+ \rightarrow l^+\nu) = \frac{G_F^2}{8\pi} f_{D_{(s)}}^2 m_l^2 M_{D_{(s)}} \left(1 - \frac{m_l^2}{M_{D_{(s)}}^2}\right) |V_{cd(s)}|^2, \quad (1)$$

where G_F is the Fermi coupling constant, f_D (f_{D_s}) is the D^+ (D_s^+) decay constant, M_D (M_{D_s}) is the D^+ (D_s^+) mass, m_l is the mass of the charged lepton, and V_{cd} (V_{cs}) is the $c \rightarrow d$ ($c \rightarrow s$)

CKM transition matrix element. These decays are helicity suppressed and, based on Eq. 1, the SM predicts $\Gamma(D^+ \rightarrow l^+\nu) = 2.3 \times 10^{-5} : 1 : 2.64$ and $\Gamma(D_s^+ \rightarrow l^+\nu) = 2.3 \times 10^{-5} : 1 : 9.72$, with $l = e : \mu : \tau$, respectively. Deviations from these predictions may arise from physics beyond the SM. Recent measurements of leptonic decays of the D^+ and D_s^+ are discussed in the following subsections.

2.1. $D^+ \rightarrow l^+\nu$

The BES Collaboration reported a measurement of the $D^+ \rightarrow \mu^+\nu_\mu$ branching fraction using 33 pb^{-1} of e^+e^- annihilation data collected on the $\psi(3770)$ resonance with the BES II detector [2]. Events are selected using the Mark III “ D -tagging” method [3], which consists of fully reconstructing the \bar{D} meson from $e^+e^- \rightarrow \psi(3770) \rightarrow D\bar{D}$ events and studying the D decay. In (semi)leptonic decays, the neutrino is inferred from the missing four-momentum in the event. Using a sample of 5300 tagged D^- decays (note that charge conjugation is implied unless otherwise stated) from 9 tag modes and requiring one additional particle consistent with a muon, 3 candidate events are observed with 0.3 background events. This leads to a branching fraction of $\mathcal{B}(D^+ \rightarrow \mu^+\nu_\mu) = (12_{-5}^{+11} \pm 1) \times 10^{-4}$, where the first error is statistical and the second is systematic.

The CLEO Collaboration reported an updated measurement of the $D^+ \rightarrow \mu^+\nu_\mu$ branching fraction [4]. Using a 281 pb^{-1} data sample collected at the $\psi(3770)$ resonance with the CLEO-c detector, a sample of 158,000 D^- decays from 6 tag modes was studied using the D -tagging method described above. Candidate events are required

to have one charged track of opposite charge to the tagged D^- and the track needs to deposit an energy in the electromagnetic calorimeter ($E_{\text{tkCC}} < 300$ MeV), which is consistent with a minimum ionizing particle. Events with an isolated photon-like shower in the calorimeter with an energy in excess of 250 MeV are rejected. Figure 1 shows the missing mass squared distribution for the candidate events, where the missing mass squared is defined as $MM^2 \equiv (E_b - E_\mu)^2 - (-\mathbf{p}_D - \mathbf{p}_\mu)^2$, where E_b is the beam energy, \mathbf{p}_D is the momentum of the tagged D^- , and E_μ (\mathbf{p}_μ) is the energy (momentum) of the muon. The signal region, defined by $|MM^2| < 0.05$ GeV^2 , contains 50 candidate and 2.8 background events, of which 1.1 events are determined from the SM prediction for $D^+ \rightarrow \tau^+ \nu_\tau, \tau^+ \rightarrow \pi^+ \bar{\nu}_\tau$. The result corresponds to $\mathcal{B}(D^+ \rightarrow \mu^+ \nu_\mu) = (4.4 \pm 0.7 \pm 0.1) \times 10^{-4}$.

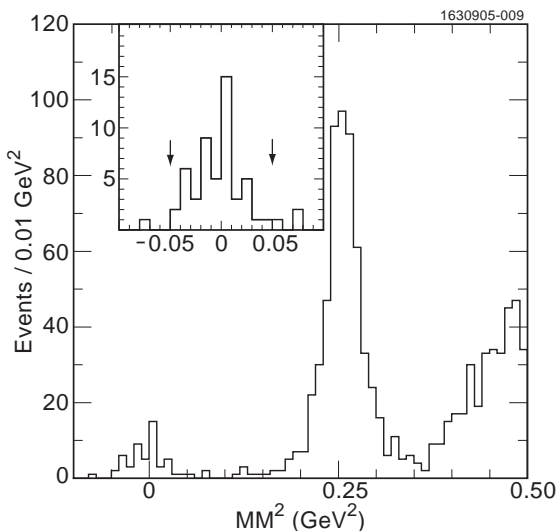


Figure 1. CLEO MM^2 distribution for $D^+ \rightarrow \mu^+ \nu_\mu$ decays [4]. The inset shows the signal region, defined by the arrows, in more detail. The background peak at $MM^2 \sim 0.25$ GeV^2 is consistent with $D^+ \rightarrow K_L^0 \pi^+$ decays and is substantially displayed from the signal region.

A complementary CLEO analysis searched for $D^+ \rightarrow e^+ \nu_e$ decays [4]. In this case, the charged track is required to be consistent with a positron. No signal is observed and an upper limit of $\mathcal{B}(D^+ \rightarrow e^+ \nu_e) < 2.4 \times 10^{-5}$ at 90% confidence level (C.L.) is obtained.

The CLEO Collaboration has reported on the search for $D^+ \rightarrow \tau^+ \nu_\tau, \tau^+ \rightarrow \pi^+ \bar{\nu}_\tau$ using the same 281 pb^{-1} and tagged D^- sample [5]. For minimum ionizing pions with $E_{\text{tkCC}} < 300$ MeV, the signal region is defined as $0.05 < MM^2 < 0.175$ GeV^2 , above $D^+ \rightarrow \mu^+ \nu_\mu$ signal region and below the $D^+ \rightarrow K_L^0 \pi^+$ background (see Fig. 1). Pions which hadronize in the calorimeter are studied by requiring the track to have $E_{\text{tkCC}} > 300$ MeV, be inconsistent with a positron, and reside in the region $-0.05 < MM^2 < 0.175$ GeV^2 . Events are rejected in both cases if it contains an isolated photon-like shower with an energy in excess of 250 MeV or if the candidate pion is more consistent with being a charged kaon. No significant enhancement is observed in either case, resulting in an upper limit of $\mathcal{B}(D^+ \rightarrow \tau^+ \nu_\tau) < 2.1 \times 10^{-3}$ (90% C.L.). Using the CLEO result for $D^+ \rightarrow \mu^+ \nu_\mu$ above, an upper limit for the ratio $\mathcal{B}(D^+ \rightarrow \tau^+ \nu_\tau) / \mathcal{B}(D^+ \rightarrow \mu^+ \nu_\mu)$ of 1.8 times that of the SM prediction is placed.

2.2. $D_s^+ \rightarrow l^+ \nu$

The BaBar Collaboration analyzed a 230.2 fb^{-1} data sample taken at or near the $\Upsilon(4S)$ resonance to study the decay process $D_s^+ \rightarrow \mu^+ \nu_\mu$ [6]. They studied the process $e^+ e^- \rightarrow D_s^{*+} D_{\text{tag}}$, where D_{tag} are 16 fully reconstructed $D^0, D^-, D_s^-,$ and D^{*-} decays and $D_s^{*+} \rightarrow \gamma D_s^+ \rightarrow \gamma(\mu^+ \nu_\mu)$, using a method similar to an earlier CLEO measurement [7]. Figure 2 shows the resultant $\Delta M \equiv M(D_s^{*+}) - M(D_s^+)$ distribution. With 489 ± 55 signal events, they determine $\Gamma(D_s^+ \rightarrow \mu^+ \nu_\mu) / \Gamma(D_s^+ \rightarrow \phi \pi^+) = 0.143 \pm 0.018 \pm 0.006$. Using the recent BaBar result $\mathcal{B}(D_s^+ \rightarrow \phi \pi^+) = (4.71 \pm 0.46)\%$ [8], they determine a branching fraction of $\mathcal{B}(D_s^+ \rightarrow \mu^+ \nu_\mu) = (0.67 \pm 0.08 \pm 0.03 \pm 0.07)\%$, where the last error arises from the $D_s^+ \rightarrow \phi \pi^+$ normalization uncertainty.

As part of the CLEO-c run plan, the energy region 3.97 - 4.26 GeV was scanned to determine

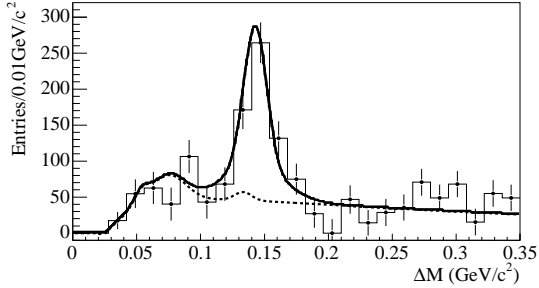


Figure 2. BaBar ΔM distribution for $D_s^+ \rightarrow \mu^+\nu_\mu$ decays [6]. The solid line is the fitted signal and background distribution, while the dashed line is the background distribution alone.

the best energy for D_s production. The energy $\sqrt{s} = 4.170$ GeV was found to be the location with the highest production rate of D_s mesons, but the D_s mesons are predominately produced in the processes $e^+e^- \rightarrow D_s^{*-}D_s^+, D_s^-D_s^{*+}$. The tagging procedure becomes more complicated by the presence of the transition photon from the radiative decay process $D_s^* \rightarrow D_s\gamma$.

Using a 195 pb^{-1} data sample collected near $\sqrt{s} = 4.170$ GeV, the CLEO Collaboration reported preliminary branching fractions for $D_s^+ \rightarrow l^+\nu$ decays, where $l = e, \mu, \tau$, and with the tau decaying via $\tau^+ \rightarrow \pi^+\bar{\nu}_\tau$ [9]. Events are selected with 8 D_s^- tag modes and the detection of the transition photon. The missing mass squared for D_s^+ is defined as $MM^2 \equiv (E_{\text{CM}} - E_{D_s} - E_\gamma - E_{\text{tk}})^2 - (-\mathbf{p}_{D_s} - \mathbf{p}_\gamma - \mathbf{p}_{\text{tk}})^2$, where E_{CM} is the center-of-mass energy, E_{D_s} (\mathbf{p}_{D_s}) is the energy (momentum) of the tagged D_s^- , E_γ (\mathbf{p}_γ) is the energy (momentum) of the transition photon, and E_{tk} (\mathbf{p}_{tk}) is the energy (momentum) of the candidate track. The signal side, consisting of one charged track, is reconstructed using the same criteria as the CLEO $D^+ \rightarrow l^+\nu$ analyses described above, but with the exceptions of increasing the $D_s^+ \rightarrow e^+\nu_e$ and $D_s^+ \rightarrow \tau^+\nu_\tau$ MM^2 signal regions to 0.20 GeV^2 and increasing the maximum shower energy to 300 MeV. Figure 3 shows the MM^2 distributions. Signals are apparent in Figs. 3i and 3ii, while no signal is observed near $MM^2 = 0$

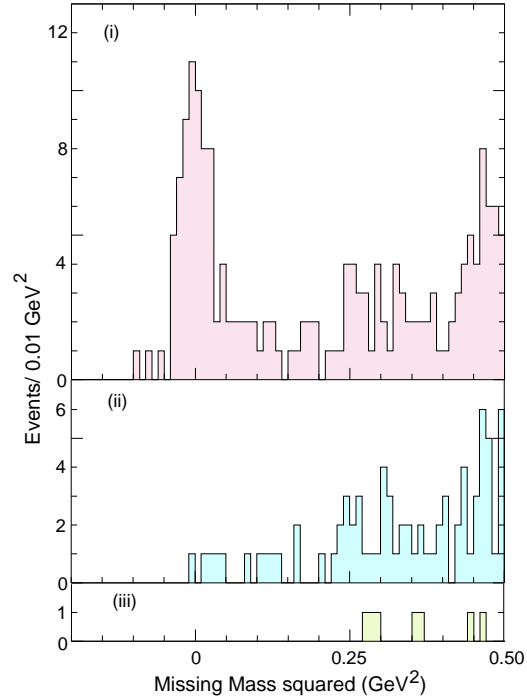


Figure 3. CLEO MM^2 distributions for $D_s^+ \rightarrow l^+\nu$ decays, where $l = e, \mu, \tau$ [9]. Figure 3i contains tracks with $E_{\text{tkCC}} < 300$ MeV, Fig. 3ii contains tracks with $E_{\text{tkCC}} > 300$ MeV and inconsistent with the positron hypothesis, while Fig. 3iii contains tracks which are consistent with the positron hypothesis.

for the positron decay channel in Fig. 3iii. The $D_s^+ \rightarrow \mu^+\nu_\mu$ signal region contains 64 candidate and 7.3 background events, of which 5.3 events are determined from the SM prediction for $D_s^+ \rightarrow \tau^+\nu_\tau, \tau^+ \rightarrow \pi^+\bar{\nu}_\tau$. Using events with candidate tracks inconsistent with the positron hypothesis and outside of the $D_s^+ \rightarrow \mu^+\nu_\mu$ signal region, 36 candidate and 4.8 background $D_s^+ \rightarrow \tau^+\nu_\tau$ events are found. The preliminary branching fractions are $\mathcal{B}(D_s^+ \rightarrow e^+\nu_e) < 3.1 \times 10^{-4}$ (90% C.L.), $\mathcal{B}(D_s^+ \rightarrow \mu^+\nu_\mu) = (0.66 \pm 0.09 \pm 0.03)\%$, and $\mathcal{B}(D_s^+ \rightarrow \tau^+\nu_\tau) = (7.1 \pm 1.4 \pm 0.3)\%$.

A complementary CLEO analysis of $\mathcal{B}(D_s^+ \rightarrow \tau^+\nu_\tau)$ was reported using the decay mode $\tau^+ \rightarrow$

Table 1

Experimental and theoretical results for the decay constants f_D and f_{D_s} .

	f_{D_s} (MeV)	f_D (MeV)	f_{D_s}/f_D
CLEO[9,10] ^a [4]	280(12)(6) ^a	222.6(16.7) ^{+2.8} _{-3.4}	1.26(11)(3) ^a
BaBar[6]	283(17)(4)(14)		
BES[2]		371 ⁺¹²⁹ ₋₁₁₇ (25)	
Unquenched LQCD[11]	249(3)(16)	201(3)(17)	1.24(1)(7)
Quenched LQCD[12]	266(10)(18)	235(8)(14)	1.13(3)(5)
Quenched LQCD[13]	236(8) ⁺¹⁷ ₋₁₄	210(10) ⁺¹⁷ ₋₁₆	1.13(2) ⁺⁴ ₋₂
Quenched LQCD[14]	231(12) ⁺⁶ ₋₁	211(14) ⁺¹⁰ ₋₁₂	1.10(2)
QCD Sum Rules[15]	205(22)	177(21)	1.16(1)(3)
QCD Sum Rules[16]	235(24)	203(23)	1.15(4)
Quark Model[17]	268	234	1.15
Quark Model[18]	248(27)	230(25)	1.08(1)
Potential Model[19]	253	241	1.05
Isospin Splittings[20]		262(29)	

^aThe CLEO f_{D_s} result is the average of the 3 preliminary measurements described in the text.

$e^+\nu_e\bar{\nu}_\tau$ [10]. This analysis reconstructs the tagged D_s^- but does not require detection of the transition photon. Events are selected with a positron with opposite charge to the tag and requires the summed energy of all isolated showers in the calorimeter ($E_{CC}^{\text{extra}} < 400$ MeV). The preliminary branching fraction is $\mathcal{B}(D_s^+ \rightarrow \tau^+\nu_\tau) = (6.3 \pm 0.8 \pm 0.5)\%$ and, while the CLEO $D_s^+ \rightarrow \tau^+\nu_\tau, \tau^+ \rightarrow \pi^+\bar{\nu}_\tau$ analysis has smaller systematic uncertainty, this result has a smaller statistical uncertainty.

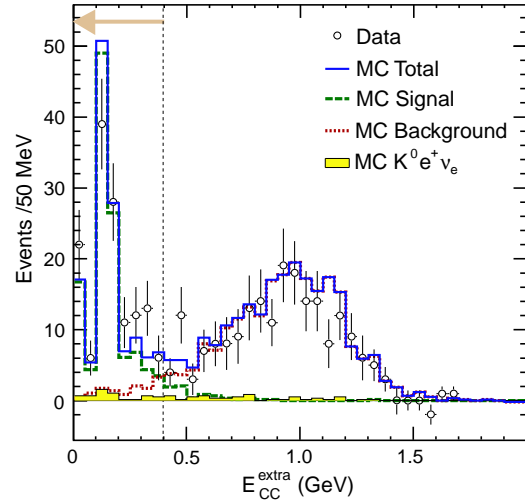
2.3. Decay Constants f_D and f_{D_s}

Table 1 summarizes the experimental results for f_D and f_{D_s} along with various theoretical predictions. The experimental results are consistent with most theoretical models. The decay constant ratio from the CLEO results is $f_{D_s}/f_D = 1.26 \pm 0.11 \pm 0.03$, which is consistent with the unquenched LQCD[11] prediction $1.24 \pm 0.01 \pm 0.07$ and slightly larger than other predictions.

3. SEMILEPTONIC DECAYS

3.1. Inclusive D Decays

The CLEO Collaboration reported measurements of the inclusive branching fractions for $D^0 \rightarrow X e^+\nu_e$ and $D^+ \rightarrow X e^+\nu_e$ decays and the corresponding positron momentum spectra from the 281 pb⁻¹ $\psi(3770)$ data sample [21]. The

Figure 4. E_{CC}^{extra} energy distribution from the CLEO $D_s^+ \rightarrow \tau^+\nu_\tau, \tau^+ \rightarrow e^+\nu_e\bar{\nu}_\tau$ analysis [10].

positron momentum spectra from the D^0 and D^+ decays are similar, as expected. They determine branching fractions of $\mathcal{B}(D^0 \rightarrow X e^+\nu_e) = (6.46 \pm 0.17 \pm 0.13)\%$ and $\mathcal{B}(D^+ \rightarrow X e^+\nu_e) = (16.13 \pm 0.20 \pm 0.33)\%$. After subtracting the known exclusive semileptonic decay modes [22],

Table 2

Preliminary CLEO branching fraction measurements of rare semileptonic D decays. Results are at the 10^{-4} level and upper limits are at 90% C.L.

	CLEO [23]	PDG[22]	ISGW2[24]	HQS[25]
$\mathcal{B}(D^+ \rightarrow \eta e^+ \nu_e)$	12.9(1.9)(0.7)	< 70	16 ^a	10
$\mathcal{B}(D^+ \rightarrow \eta' e^+ \nu_e)$	< 3.0	< 110	3.2 ^a	1.6
$\mathcal{B}(D^+ \rightarrow \phi e^+ \nu_e)$	< 2.0	< 209		
$\mathcal{B}(D^+ \rightarrow \omega e^+ \nu_e)$	14.9(2.7)(0.5)	16 $_{-6}^{+7}$	13	
$\mathcal{B}(D^0 \rightarrow K^- \pi^+ \pi^- e^+ \nu_e)$	2.9 $_{-1.1}^{+1.5}$ (0.5) ^b	< 12		
$\mathcal{B}(D^0 \rightarrow K_1^-(1270) e^+ \nu_e)$				
$K_1^-(1270) \rightarrow K^- \pi^+ \pi^-$) ^b	2.2 $_{-1.0}^{+1.4}$ (0.2) ^b		5.6(6) ^c	

^aPrediction assumes 10° $\eta - \eta'$ mixing angle. ^bSignal observed at a 4.5σ significance.

^cPrediction includes experimental uncertainties from $K_1^-(1270) \rightarrow K^- \pi^+ \pi^-$ decay[22].

the unobserved semileptonic branching fractions are $(0.3 \pm 0.3)\%$ and $(1.1 \pm 0.7)\%$ for the D^0 and D^+ , respectively. It is apparent that the known exclusive decays almost completely saturate the inclusive branching fractions. Combining these branching fractions with the world average for the D^{+0} lifetimes [22], the partial width ratio is $\Gamma(D^+ \rightarrow X e^+ \nu_e)/\Gamma(D^0 \rightarrow X e^+ \nu_e) = 0.985 \pm 0.028 \pm 0.015$, consistent with isospin invariance.

3.2. Rare D Decays

The CLEO Collaboration has searched for various rare semileptonic D decays with its 281 pb⁻¹ $\psi(3770)$ sample. Table 2 lists the preliminary branching fractions. With the exception of $\mathcal{B}(D^+ \rightarrow \omega e^+ \nu_e)$, these results are either first observations or improve upper limits by one order of magnitude. The results are consistent with predictions based on ISGW2 [24] and heavy quark symmetry (HQS) [25].

3.3. $D \rightarrow (\text{pseudoscalar})l^+ \nu$

Precision measurements of the $D^0 \rightarrow K^- e^+ \nu_e$ and $D^0 \rightarrow \pi^- e^+ \nu_e$ branching fractions have been measured and are listed in Table 3. The BES [27] and preliminary CLEO(Tag) [23] analyses, using 33 pb⁻¹ and 281 pb⁻¹ $\psi(3770)$ data samples, respectively, use the Mark III tagging method. An alternative CLEO analysis, CLEO(NoTag) [30], does not use the D -tagging technique but “reconstructs” the neutrino by fully reconstructing the semileptonic decay from all decay products

in the event. The Belle result [29] uses a 282 fb⁻¹ sample collected at or near the $\Upsilon(4S)$ resonance with signal events reconstructed from the decay process $D^{*+} \rightarrow D^0 \pi^+$. For comparison, a recent unquenched LQCD result is also listed in Table 3. The experimental results for $D^0 \rightarrow K^-(\pi^-)l^+ \nu$ are approaching the precision of 2% (4%), while the LQCD predictions are at the $\sim 20\%$ level.

Table 3

Branching fractions for the decays $D^0 \rightarrow K^- e^+ \nu_e$ and $D^0 \rightarrow \pi^- e^+ \nu_e$. Results are given in percent.

	$K^- e^+ \nu$	$\pi^- e^+ \nu$
PDG04[26]	3.58(18)	0.36(6)
BES[27]	3.82(40)(27)	0.33(13)(3)
CLEO-c[28] ^a	3.44(10)(10)	0.262(25)(8)
Belle[29]	3.45(10)(19)	0.279(27)(16)
CLEO(Tag) ^b	3.58(5)(5)	0.309(12)(6)
CLEO(NoTag) ^b	3.56(3)(11)	0.301(11)(10)
LQCD[31]	3.8(3)(7)	0.32(3)(7)

^aFrom a 56 pb⁻¹ sample using the D -tag technique and is a subset of the other CLEO results.

^bPreliminary results, not to be averaged.

The differential partial width for $D \rightarrow K(\pi)l^+ \nu$ decays is governed by one form factor, $f_+(q^2)$, and is given by

$$\frac{d\Gamma}{dq^2} = \frac{G_F^2}{24\pi^3} p_{K(\pi)}^3 |V_{cs(d)}|^2 \left| f_+^{K(\pi)}(q^2) \right|^2, \quad (2)$$

Table 4

Simple pole and modified pole fit results from $D \rightarrow K(\pi)l^+\nu$ decays.

	$m_{pole}^{D \rightarrow K}$ (GeV)	$m_{pole}^{D \rightarrow \pi}$ (GeV)	$\alpha^{D \rightarrow K}$	$\alpha^{D \rightarrow \pi}$
FOCUS[35]	1.93(5)(3)	1.91 $^{+0.30}_{-0.15}$ (7)	0.28(8)(7)	
CLEO III[36]	1.89(5) $^{+0.04}_{-0.03}$	1.86 $^{+0.10+0.30}_{-0.06-0.03}$	0.36(10) $^{+0.03}_{-0.07}$	0.37 $^{+0.20}_{-0.31}$ (15)
BaBar[37] ^a	1.854(16)(20)		0.43(3)(4)	
Belle[29]	1.82(4)(3)	1.97(8)(4)	0.52(8)(6)	0.10(21)(10)
CLEO-c(Tag) ^b	1.96(3)(1)	1.95(4)(2)	0.22(5)(2)	0.17(10)(5)
CLEO-c(NoTag) ^b	1.97(2)(1)	1.89(3)(1)	0.21(4)(3)	0.32(7)(3)
LQCD[31]	1.72(18)	1.99(17)	0.50(4)	0.44(4)

^aPreliminary results. ^bPreliminary results, not to be averaged.

where p_K (p_π) is the kaon (pion) momentum in the D rest frame and q^2 is the invariant mass of the lepton-neutrino pair.

Various parameterizations of the form factor have been proposed. The earliest is in terms of a simple pole model given as

$$f_+^{K(\pi)}(q^2) = \frac{f_+^{K(\pi)}(0)}{1 - q^2 / \left(m_{pole}^{D \rightarrow K(\pi)}\right)^2}, \quad (3)$$

where the pole mass is expected to be the $D^0 K^+$ ($D^0 \pi^+$) vector state $M(D_s^{*+}) = 2.112$ ($M(D^{*+}) = 2.010$) GeV. Becirevic and Kaidalov [32] proposed a modified pole model, which explicitly incorporates the $D_{(s)}^{*+}$ masses but includes a term α to account for deviations from the vector masses. Becher and Hill [33] proposed a less model-dependent way of dealing with the analytic singularities at $q^2 = m_{pole}^2$. They project the q^2 dependence into a different parameter space, which pushes the cut singularities far from the physical q^2 region, and the corresponding form factor can be represented by a rapidly converging Taylor series. Hill [34] extended the procedure to explicitly describe semileptonic D decays.

Table 4 lists the recent experimental results for the simple and modified pole variables. The FOCUS result [35] is determined from ≈ 13000 $D^{*+} \rightarrow D^0 \pi^+$ decays, where $D^0 \rightarrow K^-(\pi^-) \mu^+ \nu_\mu$. The CLEO III [36], BaBar [37], and Belle [29] results studied D^0 decays from the decay process $D^{*+} \rightarrow D^0 \pi^+$ using 7 fb^{-1} , 75 fb^{-1} , and 282 fb^{-1} data samples, respectively, collected at or near the $\Upsilon(4S)$ resonance. The preliminary CLEO results (both tagged and un-

tagged analyses) use isospin averaging of $D^0 \rightarrow K^- e^+ \nu_e$ and $D^+ \rightarrow K_S^0 e^+ \nu_e$ decays for $D \rightarrow K$ studies and $D^0 \rightarrow \pi^- e^+ \nu_e$ and $D^+ \rightarrow \pi^0 e^+ \nu_e$ decays for $D \rightarrow \pi$ studies. The recent unquenched LQCD result [31] is also listed in Table 4. The measurements of the pole masses as determined using the simple pole model are all lower than the expected vector states. The results for α are inconsistent with the null result, but present experimental accuracy does not constrain it well.

Table 5 lists recent results for $f_+^{K(\pi)}(0)$. The form factor model for CLEO results use the Hill series parameterization with three parameters, while the BES and Belle results use the modified pole model. While variations exist between the experimental results, they are consistent with the unquenched LQCD result.

Table 5

Results for the $f_+^{K(\pi)}(0)$ form factors. The form factors are similarly derived using the 2006 global fit values for V_{cs} and V_{cd} [22], with the exception of the Belle result.

	$ f_+^K(0) $	$ f_+^\pi(0) $
BES[27]	0.80(4)(3)	0.72(14)(3)
Belle[29]	0.695(7)(22)	0.624(20)(30)
CLEO(Tag) ^a	0.761(10)(7)	0.660(28)(11)
CLEO(NoTag) ^a	0.749(5)(10)	0.636(17)(13)
LQCD[31]	0.73(3)(7)	0.64(3)(6)

^aPreliminary results, not to be averaged.

Using the unquenched LQCD prediction for $f_+^{K(\pi)}(0)$ [31] allows for an experimental measure-

ment of the CKM matrix elements V_{cd} and V_{cs} . The preliminary V_{cs} result from the CLEO tagged (untagged) analysis is $V_{cs} = 1.014 \pm 0.013 \pm 0.009 \pm 0.106$ ($0.996 \pm 0.008 \pm 0.015 \pm 0.104$), where the last uncertainty arise from the theoretical uncertainty in $f_+^K(0)$. The preliminary CLEO result for V_{cd} is $0.234 \pm 0.010 \pm 0.004 \pm 0.024$ ($0.229 \pm 0.007 \pm 0.009 \pm 0.024$). For comparison, the 2006 global fit values are $V_{cs} = 0.97296 \pm 0.00024$ and $V_{cd} = 0.2271 \pm 0.0010$ [22]. The experimental uncertainties for V_{cs} and V_{cd} are at the 2% and 4% level, respectively, while the theoretical uncertainty is on the order of 10%. When future theoretical predictions achieve higher precision, semileptonic decays will be an ideal environment to precisely measure V_{cd} and V_{cs} .

3.4. $D \rightarrow (\text{vector})l^+\nu$

While the semileptonic D decays to vector mesons are an additional method to measure V_{cs} and V_{cd} , they are complicated by the presence of three form factors associated with the three helicity states of the final state meson. The spectroscopic pole dominance model proposes to parametrize the vector mesons in terms of a vector and two axial vector form factors, which are defined as

$$V(q^2) = \frac{V(0)}{1 - q^2/m_V^2}, \quad A_i(q^2) = \frac{A_i(0)}{1 - q^2/m_{A_i}^2}, \quad (4)$$

where $m_V = 2.1$ GeV and $m_{A1} = m_{A2} = 2.5$ GeV. The normalized form factors are defined by two ratios, the vector to first axial vector $R_V = V(0)/A_1(0)$ and the second to first axial vector $R_2 = A_2(0)/A_1(0)$.

3.4.1. $D \rightarrow \rho e^+\nu_e$

The CLEO Collaboration reported preliminary results for the decay processes $D^{+0} \rightarrow \rho^{0/-} e^+\nu_e \rightarrow (\pi^+\pi^{-/0})e^+\nu_e$ using the 281 pb⁻¹ $\psi(3770)$ data sample and the D -tagging technique [23]. They determine the most precise branching fractions of $\mathcal{B}(D^+ \rightarrow \rho^0 e^+\nu_e) = (2.32 \pm 0.20 \pm 0.12) \times 10^{-3}$ and $\mathcal{B}(D^0 \rightarrow \rho^- e^+\nu_e) = (1.56 \pm 0.16 \pm 0.09) \times 10^{-3}$. Using the world average for the D^{+0} lifetimes [22], they determine the partial width ratio $\Gamma(D^0 \rightarrow \rho^- e^+\nu_e)/(2 \cdot \Gamma(D^+ \rightarrow \rho^0 e^+\nu_e)) = 0.85 \pm 0.13$. They also performed a simultaneous form factor analysis of the D^0 and

D^+ decays and find $R_V = 1.40 \pm 0.25 \pm 0.03$ and $R_2 = 0.57 \pm 0.18 \pm 0.06$. This analysis represents the first form factor measurement of a Cabibbo suppressed vector decay mode in the charm system.

3.4.2. $D^+ \rightarrow \bar{K}^* l^+\nu$

The CLEO collaboration, using the 281 pb⁻¹ $\psi(3770)$ data sample and the D -tagging technique, reported a non-parametric form factor analysis using the FOCUS method [38] for the decay process $D^+ \rightarrow \bar{K}^{*0} e^+\nu_e \rightarrow (K^-\pi^+)e^+\nu_e$ [39]. CLEO confirms the presence of the s -wave interference in the $K^-\pi^+$ final state and determines results for the form factors to be consistent with the FOCUS analysis. CLEO did not observe any evidence of d - or f -wave interference in the $K^-\pi^+$ system.

4. CONCLUSION

The recent experimental results for leptonic and semileptonic decays of charm mesons are beginning to improve their accuracy to point where theoretical errors are dominating the uncertainty in the determination of the V_{cs} and V_{cd} CKM matrix elements. These measurements provide stringent tests of theoretical models, which in turn will improve the models as to lower their uncertainty but are also used to “fine-tune” the models so they can be applied with confidence to beauty leptonic and semileptonic decays. The experimental precision will continue to improve from the final CLEO-c D and D_s data samples and the beginning of data collection with the upgraded BES-III and BEPC-II facilities in 2008.

5. ACKNOWLEDGEMENTS

I wish to thank Neville Harnew, Guy Wilkinson, and all of the organizers for an engaging and enjoyable conference. This work was supported by the U.S. National Science Foundation and Department of Energy.

REFERENCES

1. D. Silverman and H. Yao, Phys. Rev. **D38** (1988) 214.

2. M. Ablikim *et al.*, BES Collaboration, Phys. Lett. **B610** (2005) 183.
3. J. Adler *et al.*, Mark III Collaboration, Phys. Rev. Lett. **62** (1989) 1821.
4. M. Artuso *et al.*, CLEO Collaboration, Phys. Rev. Lett. **95** (2005) 251801.
5. P. Rubin *et al.*, CLEO Collaboration, Phys. Rev. **D73** (2006) 112005.
6. B. Aubert *et al.*, BaBar Collaboration, arXiv:hep-ex/0607094, subm. to Phys. Rev. Lett.
7. M. Chadha *et al.*, CLEO Collaboration, Phys. Rev. **D58** (1998) 032002.
8. B. Aubert *et al.*, BaBar Collaboration, Phys. Rev. **D71** (2005) 091104.
9. M. Artuso *et al.*, CLEO Collaboration, contributed to the 33rd International Conference on High Energy Physics (ICHEP06), Moscow, Russia, arXiv:hep-ex/0607074.
10. S. Stone (CLEO Collaboration), presented at ICHEP06, Moscow, Russia, arXiv:hep-ex/0610026.
11. C. Aubin *et al.*, Fermilab Lattice, MILC, and HPQCD Collaborations, Phys. Rev. Lett. **95** (2006) 122002.
12. T.-W. Chiu *et al.*, Phys. Lett. **B624** (2005) 31.
13. L. Lellouch and C.-J. D. Lin, Phys. Rev. **D64** (2001) 094501.
14. D. Becirevic *et al.*, Phys. Rev. **D60** (1999) 074501.
15. J. Gordes, J. Penarrocha, and K. Schilcher, J. High Energy Phys. **0511** (2005) 014.
16. S. Narison, arXiv:hep-ph/020220.
17. D. Ebert, R. N. Faustov, and V. O. Galkin, Phys. Lett. **B635** (2006) 93.
18. G. Cvetic *et al.*, Phys. Lett. **B596** (2004) 84.
19. L. A. M. Salcedo *et al.*, Braz. J. Phys. **34** (2004) 297.
20. J. F. Amundson *et al.*, Phys. Rev. **D47** (1993) 3059.
21. N. E. Adam *et al.*, CLEO Collaboration, Phys. Rev. Lett. **97** (2006) 251801.
22. W.-M. Yao *et al.*, J. Phys. **G33** (2006) 1.
23. Y. Gao (CLEO Collaboration), presented at ICHEP06, Moscow, Russia.
24. D. Scora and N. Isgur, Phys. Rev. **D52** (1995) 2783.
25. S. Fajfer and J. Kamenik, Phys. Rev. **D71** (2005) 014020.
26. S. Eidelman *et al.*, Phys. Lett. **B592** (2004) 1.
27. M. Ablikim *et al.*, BES Collaboration, Phys. Lett. **B597** (2004) 39.
28. T. E. Coan *et al.*, CLEO Collaboration, Phys. Rev. Lett. **95** (2005) 181802.
29. L. Widhalm *et al.*, Belle Collaboration, Phys. Rev. Lett. **97** (2006) 061804.
30. R. Poling (CLEO Collaboration), presented at the 4th Flavor Physics and CP Violation Conference (FPCP06), Vancouver, British Columbia, Canada, arXiv:hep-ex/0606016.
31. C. Aubin *et al.*, Fermilab Lattice, MILC, and HPQCD Collaborations, Phys. Rev. Lett. **94** (2005) 011601.
32. D. Becirevic and A. B. Kaidalov, Phys. Lett. **B478** (2000) 417.
33. T. Becher and R. J. Hill, Phys. Lett. **B633** (2005) 61.
34. R. J. Hill, presented at FPCP06, Vancouver, British Columbia, Canada, arXiv:hep-ph/0606023.
35. J. M. Link *et al.*, FOCUS Collaboration, Phys. Lett. **B607** (2005) 233.
36. G. S. Huang *et al.*, CLEO Collaboration, Phys. Rev. Lett. **94** (2005) 011802.
37. B. Aubert *et al.*, BaBar Collaboration, contributed paper to ICHEP06, arXiv:hep-ex/0607077.
38. J. M. Link *et al.*, FOCUS Collaboration, Phys. Lett. **B633** (2006) 183.
39. M. R. Shepherd *et al.*, CLEO Collaboration, Phys. Rev. **D74** (2006) 052001.